

# BIOINSPIRED MICROPOROUS ELASTOMER WITH ENHANCED AND TUNABLE STRETCHABILITY FOR STRAIN SENSING DEVICE

Zongming Su<sup>1</sup>, Xuexian Chen<sup>1,3</sup>, Haotian Chen<sup>1,3</sup>, Yu Song<sup>1</sup>, Xiaoliang Cheng<sup>1</sup>, Bo Meng<sup>1,2</sup>, Zijian Song<sup>1</sup> and Haixia Zhang<sup>1,3\*</sup>

<sup>1</sup>Institute of Microelectronics, Peking University, Beijing, 100871, CHINA

<sup>2</sup>Beijing Micro Energy technology CO., LTD, Beijing, 100080, CHINA

<sup>3</sup>Academy for Advanced Interdisciplinary Studies, Peking University, Beijing, CHINA

## ABSTRACT

In this paper, we report a large-area, microporous polydimethylsiloxane (M-PDMS) membrane with maximum enhancement of fracture strain by 210% over the bulk PDMS (B-PDMS) film. The three-dimensional microporous structures, which contributes to the stretchability enhancement by underlying physical analysis, are fabricated by removing monodisperse polystyrene (PS) sphere arrays in PDMS matrix. Integrated with the capacitive strain sensor, the as-fabricated M-PDMS membrane is demonstrated as stretchable substrate for large or even extreme strain detection and human motion recognition.

## INTRODUCTION

The fabrication of electronics on flexible, soft and elastomeric substrates has paved the way for many new and exciting applications, such as e-skins [1-3], stretchable light-emitting devices [4-5], and stretchable actuators [6-7], which put forward great demands for stretchability properties of materials. As the inorganic materials, which are commonly used in traditional integrated circuits (IC), are brittle and stiff, they can hardly be used in stretchable electronics. Recently, there are many strategies for stretchability enhancement beyond intrinsic limits of these materials. The most promising approach suggests bonding stiff and inorganic materials onto the pre-straining elastomers and forming ‘wave’ micro- or nano-structures [8-11], which provides great enhancement compared to the initial limits of the functional materials.

For the substrate material, which holds all the electronics, requires even greater stretchability for the stability of the device. With large yield strength, small Young’s Modulus and high transparency, PDMS is commonly used. Even though, intrinsic limit of bulk PDMS restricts further improvement of its stretchability. For instance, 90μm PDMS film (10:1) curing at 60 °C breaks at around 100% elongation [12], resulting in the failure of electronic circuits on it. In nature world, the tongues of some lizards have attracted our attention. The microstructured muscle in their tongue, which can release strain in its elongation, greatly inspired us. Because of the special muscle fiber networks in middle part of its tongue, it can extend to more than twice over its body length for prey capture [13]. If the microstructures can enhance the stretchability of its tongue, they can also work in elastomer membrane.

In this work, we demonstrate the microporous structure for stretchability enhancement in elastomer. The maximum enhancement of more than 200% has been proved in our experiments for 3 μm microspheres. The underlying physical mechanism of the enhancement has been analyzed by 3D finite element method (FEM). The as-fabricated microporous PDMS has further been proved as stretchable-enhanced substrate for the capacitive strain sensor demonstration, which has excellent linearity and can effectively detect the bending motion of human fingers.

## STRUCTURAL DESIGN

The basic idea of the fabrication method of M-PDMS based on the mix of PS microspheres and PDMS matrix, as well as the following removal of PS spheres resulting in the formation of porous PDMS membrane (Figure 1). The micro pores in PDMS matrix are introduced by micro PS spheres, whose size can be adjusted in synthesis process, ranging from nanometer to micrometer. In our experiments, two different sizes, 1 μm and 3 μm PS spheres have been used, thus the pore size is controlled in this way. Because of the capillarity and gravity in the sedimentation process of PS spheres, the PS array can easily form in hexagonal close packed (hcp) state [14]. The trapped air between each sphere is filled by PDMS material and realizing the micro pores after the removal of these PS spheres.

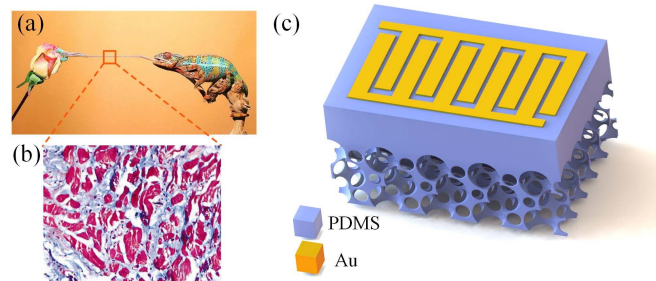


Figure 1: Bioinspired by tongue of lizard (a), the muscle fibers in its tongue (b) and 3D structure of M-PDMS strain sensor (c).

The strain sensor is designed by sputtering metal onto the pre-strained substrate, which can introduce the ‘wavy’ structure onto the metal membrane. In this way, the conductance of the sputtered metal can be reserved until the applied strain exceeds previous elongation. The specific inter-digital patterns in our experiments are controlled by a metal mask in the metal deposition process. Because of the

enhanced stretchability of the substrate, the strain sensor can work, if necessary, in a larger elongation range.

## FABRICATION PROCESS

The fabrication processes are shown in following steps: First, the PS spheres of different sizes with a concentration of 10 wt% are suspended in water and ethyl alcohol (v:v 1:1), followed by the ultra sound treatment for one hour. Then, the suspension is dipped onto the PS/glass surface, prepared by spinning coating PS solution (1 wt. % in tetrahydrofuran) on glass slice at 1000 rpm for 60 seconds and dried at 90 °C for 10 minutes. The solvent evaporates at 70 °C and leaves PS spheres onto the substrate forming the hcp array. The thickness of PS array can be adjusted by the amount of PS suspension, which is fixed in our experiment for 100 µL per square centimeter.

PDMS elastomer and cross-linker (Sylgard 184, Tow Corning) are thoroughly mixed in a 10:1 ratio (w/w), poured into the as-fabricated PS array and kept in low-pressure container (< 10 Pa) for 30 minutes. This low-pressure environment can provide a pressure gradient for the air trapped in PS array and make sure its complete replacement by liquid PDMS. A spinning coating process can be added after this process to remove redundant PDMS and obtain specific thickness of the membrane. The liquid PDMS mixture is then solidified at 90 °C for 3 hours.

Acetone acts as the solvent for PS array removal and separation of as-fabricated membrane and glass slice, which explains the choice of PS as the sacrifice layer sandwiched between the sample and the glass. The dissolution process takes 6 hours for entire removal of PS array, after which the sample is dried on hot plate for 1 hour at 60 °C. In this way, M-PDMS membrane can be fabricated.

M-PDMS consists of two parts: one is porous and another is flat. According to the above steps, the thickness of porous part can be designed, as the amount of PS spheres can be manually adjusted. Besides, the thickness of flat part can

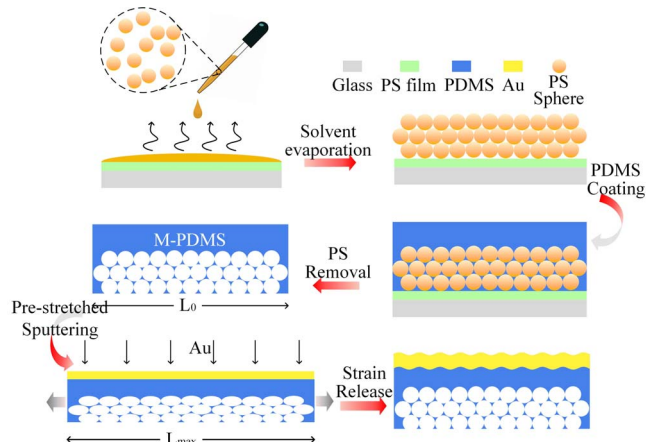


**Figure 2:** Fabrication process of M-PDMS strain sensor. Three steps are involved: the PS sedimentation, PS removal and Au sputtering

be changed by spinning speed in the fabrication process. That is to say, both of the two part can be altered, as well as the ratio of these two part. In addition, the pore size and the porous ratio in M-PDMS can be altered in the fabrication process. Thus, there are many dimensions to change the performance of the membrane.

The functional layer, capacitive sensing layer in this work, can be sputtered onto the surface of pre-strained PDMS membrane. The elongation of the pre-strain, which is set as 40 percent in this demonstration, can be adjusted on demand. After the sputtering process, the strain is released from the substrate and forming the ‘wavy’ microstructures onto the metal layer (gold in this case) because the shear stress caused by highly inconsistent stretchability between sputtered metal and substrate. In this way, the capacitive sensing part can be integrated with M-PDMS.

## RESULTS AND DISCUSSION

### Modeling and Simulation

An analytical mechanics model has been developed to analyze the strain distribution of M-PDMS. SolidWorks software is utilized for the modeling process of B-PDMS and M-PDMS structures, in which the size of each structure is based on the experimental data. After the modeling, the both structures are imported into the simulation software (Comsol Multiphysics) for the mechanical analysis. The simulated results of strain distribution are compared for B-PDMS and M-PDMS at different elongation level (0%, 50% and 100% elongation) in Figure 3. The apparent difference of the two models is that the strain of B-PDMS changes little at different positions; however, the strain of M-PDMS can be distributed to the microstructures. For the material with microstructures, the elongation process takes two steps. First, the microstructures tend to deform when external force applied. This process will not stop until the connectors of the microstructure has been straightened. Second, the deformed structure stretches driven by the external force, just like the process of B-PDMS.

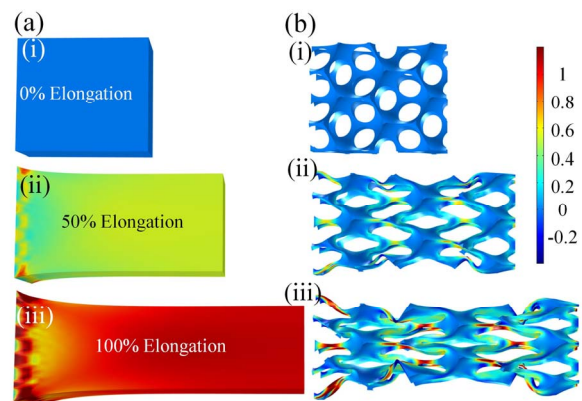


**Figure 3:** Different strain distribution of B-PDMS (a) and M-PDMS (b) under different elongations ((i).0%, (ii).50% and (iii).100%) by 3D finite element analysis.

Because of the introduction of micro pores into the PDMS membrane, the strain in the elongation can be easily dispersed and the break point can be greatly set back, which can explain the enhanced stretchability of M-PDMS.

### Morphology of M-PDMS

The optical and scanning electron microscope (SEM) images of samples in several typical fabrication steps are shown in Figure 4. From (a) to (c), we show the white PS array compared with 20 cent Euro coin, the dissolution process in acetone and the strain sensor manipulated by hand, respectively. The as-fabricated M-PDMS is no longer transparent, as the micro pores in the matrix reflect most incident light. The SEM photo of PS array (Figure 4d) shows the top two sphere layers have perfect hcp lattices, while the down pores in M-PDMS (Figure 4e) are not as perfect as them in the top. The cross-section SEM photos of M-PDMS with 3  $\mu\text{m}$  and 1  $\mu\text{m}$  are shown in (f) and (g), respectively. The porous PDMS has an obvious boundary with the flat PDMS. Besides, the pores in M-PDMS can be easily observed.

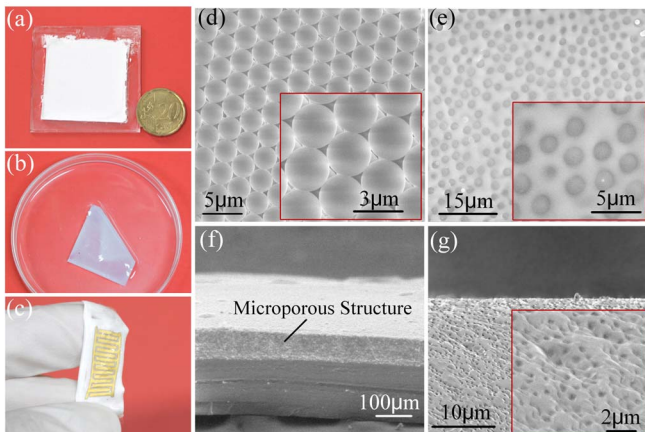


Figure 4: Optical and SEM images. (a-c): photos of PS sphere arrays, removal of PS spheres and strain sensor, (d-g): SEM of sphere arrays, microporous structure and cross section of M-PDMS with 3  $\mu\text{m}$  and 1  $\mu\text{m}$  pores, respectively.

### Stretchability Measurement

The strain-stress relationship, which reveals basic mechanical property of materials, has been tested and compared for bulk PDMS and M-PDMS with different pore sizes. The result, shown in Figure 5, proves the stretchability enhancement of M-PDMS with both pore sizes. For B-PDMS with thickness of 150  $\mu\text{m}$  breaks at 144%, while M-PDMS with 1  $\mu\text{m}$  and 3  $\mu\text{m}$  pore size break at 251% and 303%, respectively. The stretchability enhancement reaches 210% for 3  $\mu\text{m}$  – pore M-PDMS. Besides, the Young's Modulus of M-PDMS has diminished from 2MPa for B-PDMS to 0.3MPa for 1  $\mu\text{m}$  pore M-PDMS. Because the PS sphere array occupies about 74% space calculated by hcp model, the loss of such large amount of PDMS mass in the porous region can explain the decrease of Young's Modulus. However, the explanation of the highly enhanced yield strength is not so

obvious. Thus, we set up an inversed hcp model for 3D FEM simulation to explain how microstructure change can influence the stretchability enhancement of M-PDMS.

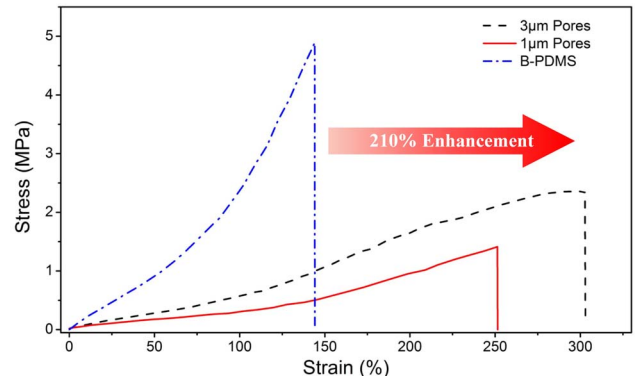


Figure 5: Stress-strain curves of B-PDMS and M-PDMS with different pore sizes (thickness of 150  $\mu\text{m}$ ).

### Capacitive Strain Sensor

To demonstrate the stability and stretchability of M-PDMS, it works as the substrate for capacitive stain sensor, of which the properties of mechanics and electronics have been tested and shown in Figure 6.

As known to all, because of the gap increase, the capacitive value of the sensor diminishes with its elongation according to the calculation formulas of capacitor. With a linear relationship between capacitive value and the gap, the sensor value decrease linearly when strain increases. The experimental results prove the theoretical analysis in Figure 6a. This excellent linearity keeps stable even at the 50<sup>th</sup>

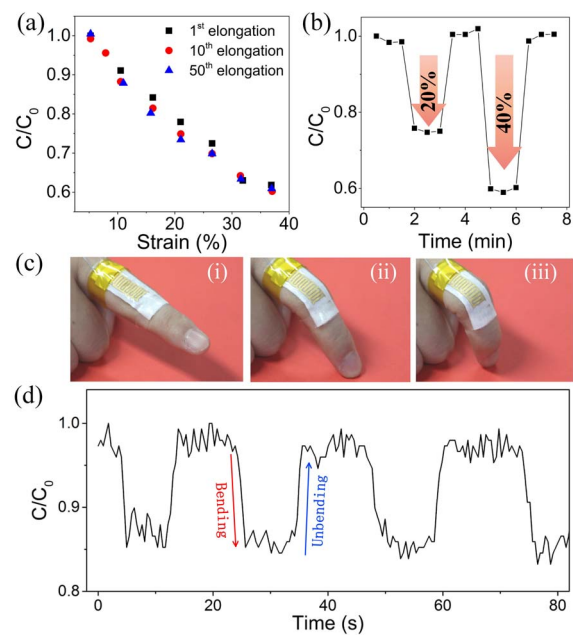


Figure 6: Strain sensing properties (a-b) under durable tests and Motion detection of human finger by M-PDMS strain sensor (c-d). The finger quickly bending and holding for 10 seconds and then quickly unbending.

elongation. The difference of 20% and 40% elongation can be easily distinguished at Figure 6b.

Because of its highly flexibility and stretchability, the capacitive strain sensor can be utilized for human motion detection. In our work, the sensor has been demonstrated on human fingers for detecting both bending and unbending motions. The device is bonded with the finger by double-side tape and tested on human finger, of which the testing photos and capacitive results are shown in Figure 6c. When the volunteer bends his finger, the capacitance of the sensor has specific change. Before unbending, the finger holds on for about 10 seconds, during which the capacitance keeps stable. The strain can recover to its original state after its unbending motion, so as to the capacitance of the sensor. The bending and unbending processes promote alternatively, and result in the change and recover of the capacitive strain sensor, accordingly. Because of its high durability, the sensor works well during human's motion.

## CONCLUSIONS

Inspired by muscle fiber networks in tongue of lizard, we promote a novel approach to fabricate microporous elastomer, which has enhanced stretchability greatly. The underlying mechanics have been analyzed by FEA tools. This stretchability enhancement provides more possibility for stretchable electronics. To demonstrate its usage for electronic device, the as-fabricated M-PDMS acts as the substrate of a capacitive strain sensor. The sensor has excellent linearity and durability to detect strain from 0% to 40%, which has been used to test human motion effectively in our experiments. This demonstration shows great possibility for M-PDMS used in future stretchable electronics.

## ACKNOWLEDGEMENTS

This work is supported by the National Natural Science Foundation of China (Grant No. 61674004, 61176103 and 91323304), National Key R&D Project from Minister of Science and Technology, China (2016YFA0202701), and the Beijing Science & Technology Project (Grant No. Z141100003814003) and the Beijing Natural Science Foundation of China (Grant No. 4141002).

## REFERENCES

- [1] M. L. Hammock, A. Chortos, *et al.* “25th Anniversary Article: The Evolution of Electronic Skin (E-Skin): A Brief History, Design Considerations, and Recent Progress”, *Adv. Mater.*, vol. 25, pp. 5997-6038, 2013.
- [2] N. Lu, C. Lu, S. Yang, *et al.* “Highly Sensitive Skin-Mountable Strain Gauges Based Entirely on Elastomers”. *Adv. Funct. Mater.*, vol. 22, pp. 4044-4050, 2012.
- [3] D. P. J. Cotton, I. M. Graz, S. É. P. Lacour. “A multifunctional capacitive sensor for stretchable electronic skins”. *IEEE Sensors Journal*, vol. 9, pp. 2008-2009, 2009.
- [4] H. L. Filiatrault, G. C. Porteous, R. S. Carmichael, *et al.* “Stretchable light-emitting electrochemical cells using an elastomeric emissive material”. *Adv. Mater.*, vol. 24, pp. 2673-2678, 2012.
- [5] Z. Yu, X. Niu, Z. Liu, *et al.* “Intrinsically Stretchable Polymer Light-Emitting Devices Using Carbon Nanotube-Polymer Composite Electrodes”. *Adv. Mater.*, vol. 23, pp. 3989-3994, 2011.
- [6] C. Keplinger, J. Y. Sun, C. C. Foo, *et al.* “Stretchable, transparent, ionic conductors”. *Science*, vol. 341, pp. 984-987, 2013.
- [7] S. Rosset, H. R. Shea. “Flexible and stretchable electrodes for dielectric elastomer actuators”. *Appl. Phys. A*, vol. 110, pp. 281-307, 2013.
- [8] J. A. Rogers, T. Someya, Y. Huang. “Materials and mechanics for stretchable electronics”. *Science*, vol. 327, pp. 1603-1607, 2010.
- [9] C. Yu, Z. Wang, H. Yu, *et al.* “A stretchable temperature sensor based on elastically buckled thin film devices on elastomeric substrates”. *Appl. Phys. Lett.*, vol. 95, 141912, 2009.
- [10] M. Gonzalez, F. Axisa, M. V. Bulcke, *et al.* “Design of metal interconnects for stretchable electronic circuits”. *Microelectron. Reliab.*, vol. 48, pp. 825-832, 2008.
- [11] D. Qi, Z. Liu, M. Yu, *et al.* “Highly stretchable gold nanobelts with sinusoidal structures for recording electrocorticograms”. *Adv. Mater.*, vol. 27, pp. 3145-3151, 2015.
- [12] J. Park, S. Wang, M. Li, *et al.* “Three-dimensional nanonetworks for giant stretchability in dielectrics and conductors”. *Nat. Commun.*, vol. 3, 916, 2012.
- [13] C. Chamaeleon. “Functional Anatomical, Histological and Ultrastructural Studies of three Chameleon Species: Chamaeleo Chamaeleon, Chamaeleo Africanus, and Chamaeleon Vulgaris”. *Int. J. Morphol.*, vol. 33, pp. 1045-1053, 2015.
- [14] Y. H. Ye, F. LeBlanc, A. Haché, *et al.* “Self-assembling three-dimensional colloidal photonic crystal structure with high crystalline quality”. *Appl. Phys. Lett.*, vol. 78, pp. 52-54, 2001.

## CONTACT

\*H. X. Zhang, tel: +86-10-62767742;  
zhang-alice@pku.edu.cn